ACS Partner Journal

Journal of the American Society for Mass Spectrometry

pubs.acs.org/jasms

Research Article

The Wisconsin Oscillator: A Low-Cost Circuit for Powering Ion Guides, Funnels, and Traps

Steven J. Kregel,* Blaise J. Thompson, Gilbert M. Nathanson, and Timothy H. Bertram

Cite This: *J. Am. Soc. Mass Spectrom.* 2021, 32, 2821−2826

Read Online

ACCESS | Metrics & More | Article Recommendations | Supporting Information

ABSTRACT: In this work, we present the Wisconsin Oscillator, a small, inexpensive, low-power circuit for powering ion-guiding devices such as multipole ion guides, ion funnels, active ion-mobility devices, and non-mass-selective ion traps. The circuit can be constructed for under $30 and produces two antiphase RF waveforms of up to 250 V_{p-p} in the high kilohertz to low megahertz range while drawing less than 1 W of power. The output amplitude is determined by a 0−6.5 VDC drive voltage, and voltage amplification is achieved using a resonant LC circuit, negating the need for a large RF transformer. The Wisconsin Oscillator automatically oscillates with maximum amplitude at the resonant frequency defined by the onboard capacitors, inductors, and the capacitive load of the ion-guiding device. We show that our circuit can replace larger and more expensive RF power supplies without degradation of the ion signal and expect this circuit to be of use in miniature and portable mass spectrometers as well as in home-built systems utilizing ion-guiding devices.

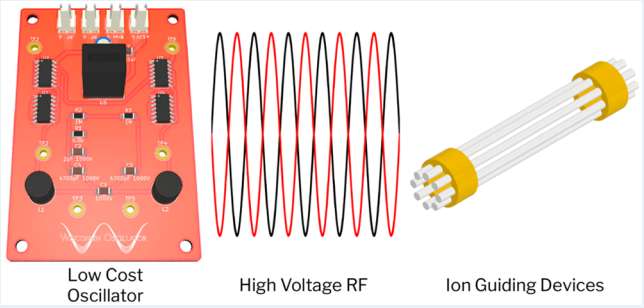

INTRODUCTION

Devices requiring high voltage RF waveforms are utilized extensively within mass spectrometers to manipulate ions in a non-mass-selective manner, typically for the purpose of transporting them between different pressure regions. These devices include ion funnels[1] and multipole ion guides[2] as well as active ion-mobility devices.[3,4] The theory of ion motion in inhomogeneous RF fields has been exquisitely laid out by Gerlich[5] and stipulates that devices designed for manipulating ions in the mass range of small molecules and polypeptides be driven with RF waveforms in the high kilohertz to low megahertz regime and a few hundred volts peak to peak. Unlike the more stringent requirements for driving a mass-selective quadrupole, these requirements are general guidelines and depend on the specific geometry of the ion-guiding device, with a wide range of voltages and frequencies providing high transmission for ions in a given mass window. While commercial instruments contain all the hardware necessary for operating their ion-guiding devices, home-built instruments must source these electronics themselves. The high cost of purchasing these supplies (~$5k−$20k/unit), and the fact that each device requires its own driving circuitry renders these commercial circuits out of reach for many academic research groups whose instruments may require multiple supplies.[6−12]

Multiple groups have reported circuits for low cost (<$500) multipole power supplies with varying degrees of accessibility and applicability to ion transport.[13,14] The designs of O'Connor[15,16] and Jau[17] remove the necessity of frequency and impedance matching by automatically oscillating at the frequency defined by the capacitance of the ion-guiding device, while the O'Connor and Noriega[18] circuits both contain mechanisms for amplitude control through a 0−10 VDC signal. Although these supplies all provide the requisite frequency and amplitude characteristics, they suffer from some drawbacks. The Jau and Noriega circuits are designed to drive 3D ion traps and produce only a single phase of RF output, which is unsuitable for devices designed for ion transport, where the net electric field applied to the device must remain fixed. The O'Connor design produces antiphase output, but it requires the careful construction of a custom multiwinding air-core transformer in which small imperfections can result in drastic changes to the RF output, making it difficult to dial in a specific frequency. Additionally, some components in the O'Connor design normally operate near their damage threshold, and accidental overdriving of this circuit (an unfortunately common occurrence during the construction of home-built instrumentation) can result in destruction of the power supply. Historically, the large air-core transformers used for stepping up RF voltages have frustrated the efforts to develop miniature mass spectrometers.[19] A few

Received: August 18, 2021
Revised: October 19, 2021
Accepted: October 19, 2021
Published: November 3, 2021

Downloaded via UNIV OF WISCONSIN-MADISON on April 1, 2024 at 20:39:16 (UTC).
See https://pubs.acs.org/sharingguidelines for options on how to legitimately share published articles.

ACS Publications

© 2021 American Society for Mass Spectrometry. Published by American Chemical Society. All rights reserved.

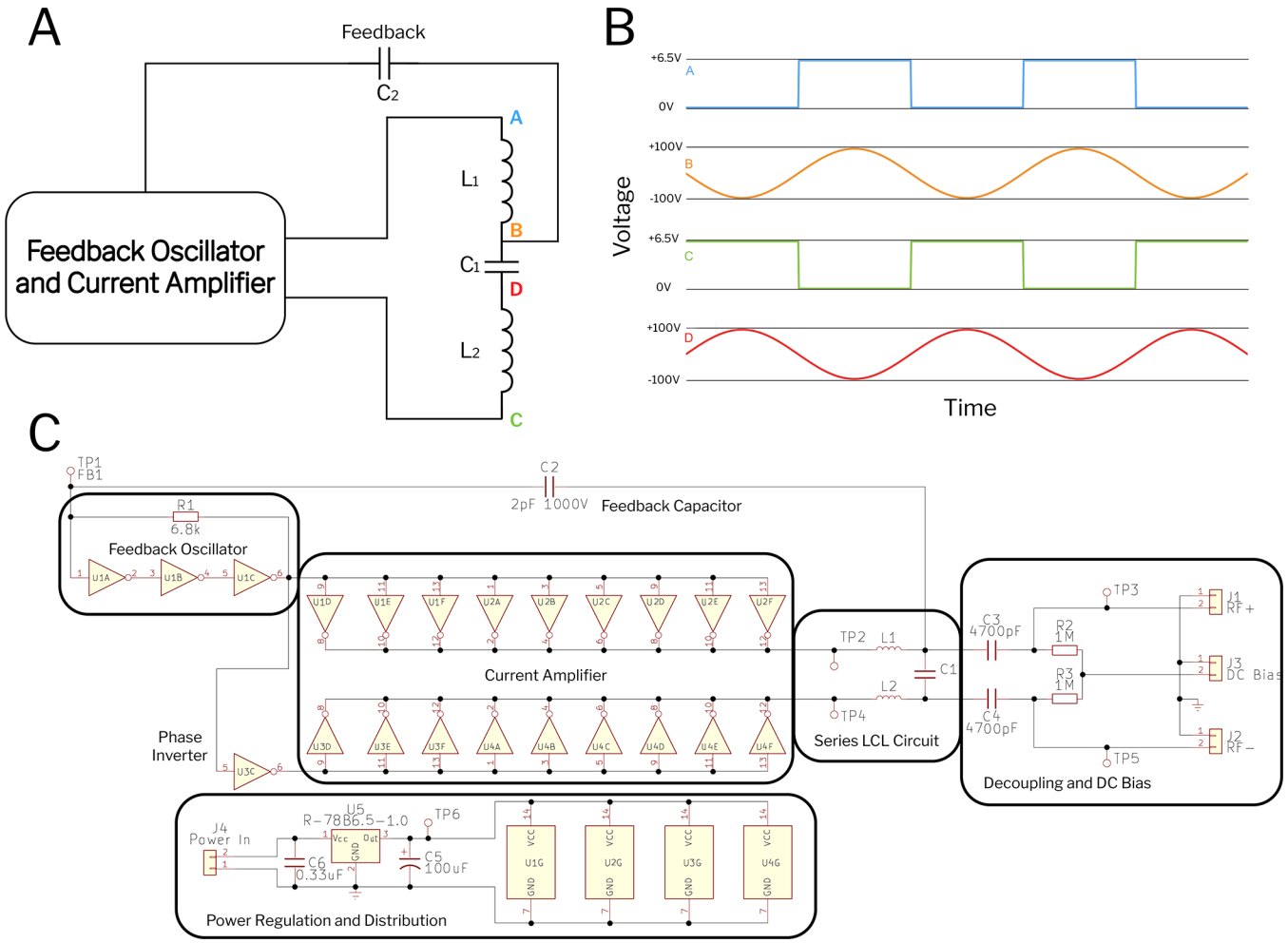

Figure 1. (A) Conceptual schematic of the series LCL circuit and feedback mechanism. (B) The phase relationship of voltages at selected points. (C) Full schematic of the circuit.

groups have experimented with using square waves to drive ion-guiding devices.[20,21] While more flexible than sine waves in that the oscillation frequency can be easily varied, powering the ion-guiding device with square waves is inherently a non-resonant process requiring a large power draw and is therefore unsuitable for many miniature and field deployable applications.

In this work, we present the design and construction of the Wisconsin Oscillator, a small, inexpensive, and robust RF power supply for powering ion-guiding devices. The circuit is contained within a 50.8 mm × 76.2 mm (2" × 3") footprint and constructed entirely with off the shelf components totaling less than $20 without requiring a transformer. It is powered by an external 12 VDC power supply and draws less than 1 W of power. Additionally, it requires no impedance matching to produce two antiphase RF signals of up to 250 V_{p-p} in the high kilohertz to low megahertz range, which float on top of a DC bias and whose frequency can be easily altered by replacing the onboard inductors or capacitors.

CIRCUIT DESCRIPTION

The design of the Wisconsin Oscillator was inspired by that of Jau et al., who switched the driving current through a series LC circuit to induce flyback voltage pulses in-phase with the resonant LC oscillation. Their circuit produced a single phase of RF output which they used to drive an ion trap in a miniature atomic clock.[17]

The LCL Circuit. To provide the antiphase RF output suitable for ion-guiding devices, we modified the LC circuit of Jau by adding an additional inductor and driving both inductors with antiphase low voltage square waves. A functional diagram of this circuit is shown in Figure 1A, and the full schematic is presented in Figure 1C. By decoupling the capacitor (C_1) from ground, the additional inductor (L_2) allows both poles of the capacitor to oscillate, thus providing antiphase high voltage RF output as seen in Figure 1B. The combined LCL circuit oscillates at the frequency

$$f_0 = \frac{1}{2\pi\sqrt{C_{\text{total}}(L_1 + L_2)}} \quad (1)$$

where L_1 and L_2 are the values of the two inductors and C_{total} is the total capacitive load seen by the circuit, including C_1, the feedback capacitor C_2, the gate capacitance of the feedback oscillator, and the capacitive load exhibited by the ion-guiding device itself. By setting $L_1 = L_2 = \frac{L_{\text{Jau}}}{2}$ we maintain the oscillation frequency of the Jau design, while producing the required antiphase output. However, by splitting the total inductance across two inductors, we halve the RF amplitude attainable, as the flyback voltage magnitude depends on the current change through a single inductor. To correct this

https://doi.org/10.1021/jasms.1c00247
J. Am. Soc. Mass Spectrom. 2021, 32, 2821−2826

problem and recover the lost amplitude we drive current through L_2 using a second current amplifier driven 180° out of phase with respect to the drive current through L_1, as illustrated in Figure 1B. We note that a trimmable capacitor in parallel with C_1 would enable fine-tuning of the oscillation frequency. However, we have found that simply choosing an appropriate static capacitance for C_1 is sufficient, as the exact frequency is not typically important in ion-guiding applications.

Feedback Oscillator and Current Amplification. The feedback oscillator and current amplification stages are responsible for sensing the phase of the RF energy oscillating in the LCL subcircuit and switching the current through L_1 and L_2 at the RF zero crossings. This sudden change in current induces flyback voltage spikes in-phase with the RF oscillation. As the inverter gates can source and sink identical values of current, the input sides of the inductor (points A and C in Figure 1A) are constrained to the voltage determined by the inverter, and the flyback voltage is generated exclusively between the inductors and C_1 (points B and D in Figure 1A). The feedback oscillator consists of three inverter gates with a feedback resistor, R_1. The three inverters in series serve to increase the gain, enabling the circuit to more rapidly reach its equilibrium operating condition compared to a feedback oscillator comprising a single inverter. The small feedback capacitor C_2 samples the voltage in the LCL tank to drive the input of the feedback oscillator in combination with R_1.

To maximize the induced flyback voltage, we would like the current through the inductor to be as large as possible and to switch as fast as possible, so the feedback oscillator output is fed to a bank of parallel inverter gates for current amplification. To drive the half of the LCL circuit not sampled by C_2 we send the feedback oscillator through an additional inverter gate (see the phase inverter in Figure 1C) and use it to drive the second current amplifier. We choose to use two banks of nine inverters in parallel for the current amplifiers, as inverter gates are commonly produced with six circuits per chip, and the requisite 22 inverters for the feedback oscillator, phase inverter, and two current amplifiers can be obtained with only four integrated circuits.

By monitoring the LCL tank for zero crossings and responding accordingly, the frequency of the feedback oscillator automatically adjusts to the resonant frequency of the LCL subcircuit, thus eliminating the need for the frequency and impedance matching procedures required with the tuned oscillatory circuits commonly used to power quadrupoles. Ideally, the current through L_1 and L_2 is switched at the same time as an LCL subcircuit zero crossing. However, due to the limitations of physical inverter gates there is a finite amount of propagation delay between these two events and the LCL subcircuit circuit is driven slightly off resonance. The propagation delay limits the oscillator output voltage as described by Jau,[17] though empirically we find that our choice of inverter gate leads to voltages suitable for many ion-guiding devices.

AMPLITUDE CONTROL AND DC BIAS

The magnitude of the flyback voltage (and RF output) is determined by the rate of current change through the inductors which, due to the constant rise and fall time of the inverters, is determined by the voltage supplied to the inverter gates. Our chosen inverters (CD74AC04M96) can operate over a wide range of supply voltages, providing control over the output RF amplitude. As the exact RF amplitude is not critical for ion-guiding applications, we chose to use a fixed onboard regulator for the sake of simplicity. If a variable amplitude is desired, an adjustable drive voltage can be utilized, up to the limit imposed by the inverter gates.

To enable the application of a DC potential bias to the ion-guiding device, the output of the circuit is decoupled from the LCL subcircuit through two large value capacitors, C_3 and C_4. The high capacitance of these components results in a low reactance at frequencies in the upper kilohertz and low megahertz range and enables efficient RF coupling between the LCL subcircuit and ion-guiding device. The DC bias is introduced between the decoupling capacitors and the ion-guiding device through the large value resistors R_2 and R_3 which prevent the RF signal from propagating into the DC supply.

PHYSICAL CONSTRUCTION

For construction of the circuit, we designed a custom printed circuit board and enclosure. The board measures 50.8 mm × 76.2 mm (2" × 3") and includes the feedback oscillator and current amplifiers, as well as the LCL subcircuit, decoupling electronics, and voltage regulator. For reference a picture is shown in Figure 2; fabrication files and a bill of materials can

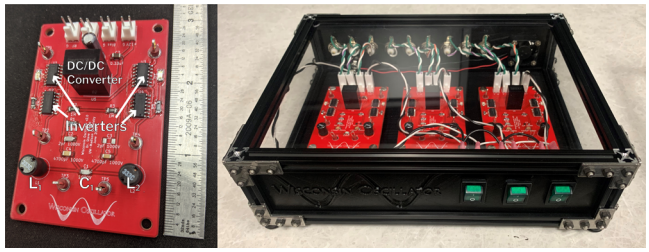

Figure 2. Photographs of an individual Wisconsin Oscillator circuit (left) and an assembled enclosure containing three separate Wisconsin Oscillators (right).

be found in the Supporting Information. For the inverter gates we use four CD74AC04M96 integrated circuits from Texas Instruments. These chips each contain six inverter gates and can operate over a wide input voltage range of 1.5−6.5 V. Each inverter gate can source and sink up to 24 mA of current with a 5 V drive, resulting in ∼215 mA from the current amplifier. However, we drive the inverter gates at their maximum supply voltage, so the actual output current is higher. Additionally, these chips have a manufacturer quoted propagation delay of 6.5 ns at 5 V drive, ensuring that the current through L_1 and L_2 is switched with minimal phase shift.

For all passive components except the inductors, we chose to use the 1206 package of surface mount components due to its good combination of small size and ease of soldering. All capacitors are rated to 1000 V, with the feedback capacitor C_2 having a capacitance of 2.2pF. For this work, we explored a variety of different values for C_1 and found that values between 50 and 100 pF work well. If desired, the value of C_1 can be changed to tune the frequency of the circuit in accordance with eq 1. The decoupling capacitors C_3 and C_4 have values of 4700 pF to minimize the reactive load and prevent attenuation of the output signal, while the bias resistors R_2 and R_3 are valued at 1 MΩ, providing sufficient DC current to bias the ion-guiding device while preventing the RF oscillations from reaching the DC power supply. The feedback resistor R_1 has a value of 6.8

https://doi.org/10.1021/jasms.1c00247
J. Am. Soc. Mass Spectrom. 2021, 32, 2821−2826

kΩ and is rated for 1/4 W. This value is an empirical compromise between allowing the buildup of oscillations and minimization of the power lost through R_1 as described in Jau.[17] For the inductors, L_1 and L_2, we chose to utilize the 2200R series of through-hole inductors from MuRata Power Solutions due to the wide range of available inductance values and high-quality factors. See Table 1 for the values of inductors used for this work. These inductors have maximum DC current ratings on par with the maximum current available from the current amplifier, and quality factors >90 for all the tested inductance values. The inductors were placed on opposite sides of the circuit board to minimize the interference of their magnetic fields during circuit operation.

Table 1. Circuit Behavior with Varying Inductance Values[a]

	no load		simulated load	
total inductance (uH, $L_1 = L_2$)	frequency (kHz)	amplitude (V_{p-p})	frequency (kHz)	amplitude (V_{p-p})
66	1780	190	1640	198
132	1260	220	1160	226
200	1020	220	930	224
400	730	240	664	242

[a]All data was acquired with C_1 = 100 pF.

Power is supplied to the board through a 12 VDC wall plug adaptor and stepped down to 6.5 VDC by the onboard DC/DC converter (RECOM Power, R-78B6.5−1.0). We use a 6.5 VDC source as this provides the maximum output amplitude within the limit imposed by the inverter chips. For the sake of simplicity, we decided to forego the ability to vary the output amplitude, but it would be simple to replace our 6.5 VDC source with a variable DC supply to provide amplitude control if needed. However, we note that unlike previous designs for RF oscillators, our circuit has no amplitude feedback mechanism and the relationship between drive voltage and output amplitude would need to be empirically determined, complicating the construction and operation of the circuit.

RESULTS AND DISCUSSION

To characterize the performance of our circuit we systematically varied the values of L_1 and L_2 to explore the achievable RF frequencies and amplitudes. All experiments were conducted using the onboard 6.5 V DC/DC converter, which as noted previously is the limit imposed by the inverter chips. The capacitive load presented by an ion-guiding device was simulated by coupling each output to ground through a separate 56 pF capacitor. As expected from eq 1, the oscillation frequency of the circuit decreased both upon addition of the capacitive load and from an increase in total inductance. While larger inductances lowered the oscillation frequency, they also resulted in larger RF amplitudes which may be desirable in some situations. The results of varying inductances are shown in Table 1. We note that these values were measured with C_1 = 100 pF, and reducing the capacitance of C_1 will serve to increase the oscillation frequency. A typical output waveform is presented in Figure 3 and shows the antiphase output of the two waveforms. As seen in the bottom panel of Figure 3, the output of the circuit contains minimal contributions from higher harmonics.

The Wisconsin Oscillator begins oscillating by amplifying the resonant frequency component of the random electrical noise omnipresent in the circuit. However, the total turn on time of the circuit contains overhead while the DC/DC converter is coming to equilibrium. To measure the inherent turn on time of the oscillator portion of the circuit we applied power directly to TP6, bypassing C_5 (100 μF) and the DC/DC converter. The oscillator reached its equilibrium operating condition ∼50 μs after direct application of power, and upon removal of power from TP6, the oscillations ceased within ∼10 μs. This fast turn on/turn off time could enable future versions of the Wisconsin Oscillator to incorporate a keying circuit, allowing the RF oscillations to be modulated during an experiment, reducing the effect of RF noise in other regions of the mass spectrometer.

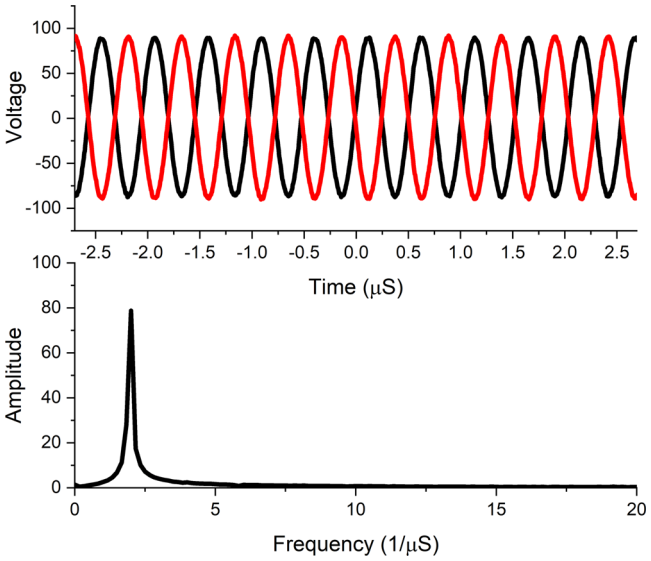

Figure 3. Output waveform with $L_1 = L_2$ = 33 μH and C_1 = 100 pF (first line of Table 1) in the time domain (top) and frequency domain (bottom).

Another feature of our design is that due to the capacitive output coupling, the outputs are protected from accidental short circuits. During testing the outputs were intentionally shorted together while the circuit was powered. As expected, the output waveform collapsed to the DC bias voltage, but upon removal of the short the RF waveform returned to its original amplitude and frequency. Additionally, as the Wisconsin Oscillator does not utilize a transformer, operation of multiple circuits within the same enclosure did not impact the output amplitude or frequency of any of the circuits.

An important consideration when designing equipment for field deployment is the total power draw of the instrument. We measured the power draw from the 12 VDC power supply to be 875 mW, with 225 mW being utilized by the 6.5 V DC/DC converter and 650 mW being utilized by the circuit itself. To calculate the intrinsic efficiency of our circuit we calculate the power required to drive the capacitive load by

$$P_R = \frac{2\pi f_0 C V_{RF}^2}{2Q} \quad (2)$$

where Q is the quality factor of the LCL circuit. At these frequencies, Q is primarily determined by the inductor, and we utilize the manufacturer quoted Q value for our calculations. In the case of 1640 kHz, 200 V_{p-p} and the 112 pF simulated load we calculate an RF power of 0.26 W for a Q = 90. This yields an efficiency of 40%, about half that obtained by Jau.[17] This is expected given our dual current amplifiers, which would

https://doi.org/10.1021/jasms.1c00247
J. Am. Soc. Mass Spectrom. 2021, 32, 2821−2826

approximately double the power required for the same peak to peak voltage.

As a definitive test of the Wisconsin Oscillator, we used five copies of the circuit to guide hydrated clusters of protonated trialanine ions through a cryogenic ion vibrational spectrometer, which contains four hexapole ion guides and an octupolar cryogenic ion trap.[7] The formation of water clusters and their transmission through the instrument show that the Wisconsin Oscillator can softly transport polypeptide ions and weakly bound clusters through a variety of ion-guiding devices over a pressure range of 0.1 Torr to 1×10^{-6} Torr. Furthermore, as seen by the mass spectra in Figure 4, we show that the

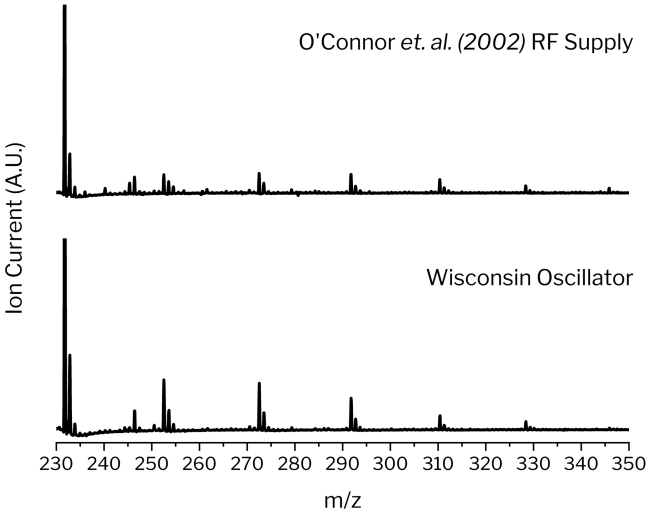

Figure 4. Mass spectra of $Ala_3H^+ \cdot (D_2O)_n$ with $n = 0-5$ taken on the Wisconsin Cryogenic Ion Vibrational Spectrometer using RF supplies based on the design of O'Connor et al. (top) and the Wisconsin Oscillator (bottom). The scales of the *y*-axes are the same in both panels.

Wisconsin Oscillator transports ions similarly to RF supplies based on the design of O'Connor[15] while being less than a quarter of the size and a tenth of the price.

CONCLUSION

In this work, we have presented a compact, robust, low-cost circuit for driving ion-guiding devices within mass spectrometers. Our circuit operates from a 12 VDC power supply and draws less than 1 W to produce antiphase RF waveforms with 250 V_{p-p} at 1 MHz with a fixed amplitude. The output waveform characteristics can be easily varied by changing the onboard inductors and capacitors, and the output is protected from accidental short circuits through capacitive coupling. In contrast to existing designs, our circuit exclusively utilizes off the shelf components, increasing its accessibility to a wider variety of researchers, and enabling the builders of custom mass spectrometers to incorporate additional ion-guiding devices without consideration of the high cost of commercial power supplies or the time commitment required for the intricate construction of previously reported circuitry. We demonstrate the applicability of our circuit by using it to replace the existing RF supplies on a home-built mass spectrometer and observing no change in ion transmission.

ASSOCIATED CONTENT

Supporting Information

The Supporting Information is available free of charge at https://pubs.acs.org/doi/10.1021/jasms.1c00247.

Fabrication files for the Wisconsin Oscillator printed circuit board and a bill of materials (ZIP)

AUTHOR INFORMATION

Corresponding Author

Steven J. Kregel − *Department of Chemistry, University of Wisconsin—Madison, Madison, Wisconsin 53706, United States;* orcid.org/0000-0001-5712-829X; Email: sjkregel@wisc.edu

Authors

Blaise J. Thompson − *Department of Chemistry, University of Wisconsin—Madison, Madison, Wisconsin 53706, United States;* orcid.org/0000-0002-3845-824X

Gilbert M. Nathanson − *Department of Chemistry, University of Wisconsin—Madison, Madison, Wisconsin 53706, United States;* orcid.org/0000-0002-6921-6841

Timothy H. Bertram − *Department of Chemistry, University of Wisconsin—Madison, Madison, Wisconsin 53706, United States;* orcid.org/0000-0002-3026-7588

Complete contact information is available at: https://pubs.acs.org/10.1021/jasms.1c00247

Notes

The authors declare no competing financial interest.

ACKNOWLEDGMENTS

This work was supported by the National Science Foundation through the National Science Foundation Center for Aerosol Impacts on Chemistry of the Environment (NSF-CAICE) under Grant No. CHE 1801971. Any opinions, findings, and conclusions of recommendations expressed in this material are those of the authors and do not necessarily reflect the views of the National Science Foundation. The authors thank Kathy Nickson, Summer Sherman, and Etienne Garand for their assistance in acquiring Figure 4.

REFERENCES

(1) Giles, K.; Pringle, S. D.; Worthington, K. R.; Little, D.; Wildgoose, J. L.; Bateman, R. H. Applications of a travelling wave-based radio-frequency-only stacked ring ion guide. *Rapid Commun. Mass Spectrom.* **2004**, *18*, 2401−2414.

(2) Javaheri, H.; Schneider, B. B. Ion Guide for Improved Atmosphere to Mass Spectrometer Vacuum Ion Transfer. *J. Am. Soc. Mass Spectrom.* **2021**, *32*, 1945−1951.

(3) Deng, L.; Webb, I. K.; Garimella, S. V. B.; Hamid, A. M.; Zheng, X.; Norheim, R. V.; Prost, S. A.; Anderson, G. A.; Sandoval, J. A.; Baker, E. S.; Ibrahim, Y. M.; Smith, R. D. Serpentine Ultralong Path with Extended Routing (SUPER) High Resolution Traveling Wave Ion Mobility-MS using Structures for Lossless Ion Manipulations. *Anal. Chem.* **2017**, *89*, 4628−4634.

(4) Guevremont, R. High-field asymmetric waveform ion mobility spectrometry: A new tool for mass spectrometry. *J. Chromatogr. A* **2004**, *1058*, 3−19.

(5) Gerlich, D. Inhomogeneous RF Fields: A Versatile Tool for the Study of Processes with Slow Ions. In *State-Selected and State-to-State Ion−Molecule Reaction Dynamics*; Ng, C.-Y., Baer, M., Eds.; John Wiley and Sons, Inc.: New York, 1992; pp 1−176.

(6) Kregel, S. J.; Thurston, G. K.; Zhou, J.; Garand, E. A multi-plate velocity-map imaging design for high-resolution photoelectron spectroscopy. *J. Chem. Phys.* **2017**, *147*, 094201.
(7) Marsh, B. M.; Voss, J. M.; Garand, E. A dual cryogenic ion trap spectrometer for the formation and characterization of solvated ionic clusters. *J. Chem. Phys.* **2015**, *143*, 204201.
(8) Wolk, A. B.; Leavitt, C. M.; Garand, E.; Johnson, M. A. Cryogenic Ion Chemistry and Spectroscopy. *Acc. Chem. Res.* **2014**, *47*, 202−210.
(9) Wang, L.-S. Perspective: Electrospray photoelectron spectroscopy: From multiply-charged anions to ultracold anions. *J. Chem. Phys.* **2015**, *143*, 40901.
(10) Hock, C.; Kim, J. B.; Weichman, M. L.; Yacovitch, T. I.; Neumark, D. M. Slow photoelectron velocity-map imaging spectroscopy of cold negative ions. *J. Chem. Phys.* **2012**, *137*, 244201.
(11) Asmis, K. R.; Brümmer, M.; Kaposta, C.; Santambrogio, G.; von Helden, G.; Meijer, G.; Rademann, K.; Wöste, L. Mass-selected infrared photodissociation spectroscopy of V4O10+. *Phys. Chem. Chem. Phys.* **2002**, *4*, 1101−1104.
(12) Rizzo, T. R.; Stearns, J. A.; Boyarkin, O. V. Spectroscopic studies of cold, gas-phase biomolecular ions. *Int. Rev. Phys. Chem.* **2009**, *28*, 481−515.
(13) Jones, R. M.; Anderson, S. L. Simplified radio-frequency generator for driving ion guides, traps, and other capacitive loads. *Rev. Sci. Instrum.* **2000**, *71*, 4335−4337.
(14) Detti, A.; De Pas, M.; Duca, L.; Perego, E.; Sias, C. A compact radiofrequency drive based on interdependent resonant circuits for precise control of ion traps. *Rev. Sci. Instrum.* **2019**, *90*, 23201.
(15) O'Connor, P. B.; Costello, C. E.; Earle, W. E. A high voltage RF oscillator for driving multipole ion guides. *J. Am. Soc. Mass Spectrom.* **2002**, *13*, 1370−1375.
(16) Mathur, R.; O'Connor, P. B. Design and implementation of a high power rf oscillator on a printed circuit board for multipole ion guides. *Rev. Sci. Instrum.* **2006**, *77*, 114101.
(17) Jau, Y.-Y.; Benito, F. M.; Partner, H.; Schwindt, P. D. D. Low power high-performance radio frequency oscillator for driving ion traps. *Rev. Sci. Instrum.* **2011**, *82*, 23118.
(18) Noriega, J. R.; García-Delgado, L. A.; Gómez-Fuentes, R.; García-Juárez, A. Low power RF amplifier circuit for ion trap applications. *Rev. Sci. Instrum.* **2016**, *87*, 94704.
(19) Snyder, D. T.; Pulliam, C. J.; Ouyang, Z.; Cooks, R. G. Miniature and Fieldable Mass Spectrometers: Recent Advances. *Anal. Chem.* **2016**, *88*, 2−29.
(20) Hoffman, N. M.; Gotlib, Z. P.; Opačić, B.; Huntley, A. P.; Moon, A. M.; Donahoe, K. E. G.; Brabeck, G. F.; Reilly, P. T. A. Digital Waveform Technology and the Next Generation of Mass Spectrometers. *J. Am. Soc. Mass Spectrom.* **2018**, *29*, 331−341.
(21) Brabeck, G. F.; Chen, H.; Hoffman, N. M.; Wang, L.; Reilly, P. T. A. Development of MSn in Digitally Operated Linear Ion Guides. *Anal. Chem.* **2014**, *86*, 7757−7763.

https://doi.org/10.1021/jasms.1c00247
J. Am. Soc. Mass Spectrom. 2021, 32, 2821−2826